

Distribution Function of Higher Harmonic ICRF Heated Plasma Calculated with Bounce-averaged Fokker-Planck Equation on LHD

SAITO Kenji, KUMAZAWA Ryuhei, MUTOH Takashi, SEKI Tetsuo, WATARI Tetsuo, TORII Yuki¹, TAKEUCHI Norio¹, SHIMPO Fujio, NOMURA Goro, YOKOTA Mitsuhiko, KATO Akemi, WATANABE Tsuguhiko, ZHAO Yangping² and LHD Experimental Group

National Institute for Fusion Science, Toki, 509-5292, Japan

¹Nagoya University, Faculty of Engineering, Nagoya, 464-8603, Japan

²Institute of Plasma Physics, Chinese Academy of Science, Hefei 230031, People's Republic of China

(Received: 9 December 2003 / Accepted: 24 March 2004)

Abstract

Higher harmonic heating is one of the effective ion cyclotron range of frequency (ICRF) heating scenarios. High-energy particles are more effectively produced by this heating method than by minority heating. To study the heating efficiency and the high-energy ion tail formation in the Large Helical Device (LHD), the distribution function was calculated using a bounce-averaged Fokker-Planck equation, and the absorbed and the lost power were estimated for the higher harmonic ICRF heating. It was found that the higher harmonic ICRF heating enhanced the D-D reaction rate.

Keywords:

higher harmonic ICRF heating, LHD, high-energy particle, bounce-averaged Fokker-Planck equation

1. Introduction

It was thought that in the helical device high-energy particles with a perpendicular pitch angle had a poor confinement performance because the trapped particle orbits are deviated from the magnetic flux surface. Ion cyclotron range of frequency (ICRF) heating was thought to work well only in the electron heating regime. However, in the Large Helical Device (LHD), the high-energy tail was observed up to 500 keV in minority ICRF heating with an inward shifted magnetic configuration [1]. In this configuration, the deviation of the orbit from the magnetic flux surface is small. For producing higher-energy particles in the LHD, a higher harmonic ICRF heating is thought to be more effective than the minority heating because under the former the particles are accelerated due to the finite Larmor radius effect. The distribution function of higher harmonic heated ions is calculated using a bounce-averaged Fokker-Planck equation to determine to which energy the ion energy is extended and to estimate the absorbed power in this heating regime. In Sec. 2, the method of calculation is introduced. In Sec. 3, calculated results are described, and Sec. 4 is a summary.

2. Calculation of Fokker-Planck equation

For simplicity of the calculation, a helical symmetrical magnetic configuration is employed as shown in Fig. 1, where the bold solid lines represent the ion cyclotron resonance layers. The plasma size is selected to be similar to that

of the LHD plasma. A wave number parallel to the magnetic line of force is assumed to be zero for simplicity. The strength of the radio frequency (rf) electric field $|E_0|$ is assumed to be constant over the whole plasma. A dispersion relation of a cold plasma approximation is used to calculate the polarity of E_0 and a wave number perpendicular to the magnetic line of force. The electron density and temperature profiles are assumed as $n_e = n_{e0}(1 - \rho^8)$ and $T_e = T_{e0}(1 - \rho^2)$, respectively, where ρ is the normalized minor radius and n_{e0} and T_{e0} are electron density and temperature on the magnetic axis, respectively. A bounce-averaged Fokker-Planck equation is obtained by integrating the local rf kick term Q and the collision term C along the magnetic line of force in the approximation of no deviation of particle-orbit from the magnetic flux surface [2].

$$\begin{aligned} \frac{\partial f_0}{\partial t} &= \bar{C}(f_0) + \bar{Q}(f_0) + S \\ \bar{C}(f_0) &= \frac{1}{\tau_b} \int \frac{dl}{v_{\parallel}} C(f_0) = \frac{1}{v^2} mv \left(\frac{\partial}{\partial E} + \frac{\mu}{E} \frac{\partial}{\partial \mu} \right) \\ &\quad \times \left[-\alpha v^2 f_0 + \frac{1}{2} mv \left(\frac{\partial}{\partial E} + \frac{\mu}{E} \frac{\partial}{\partial \mu} \right) (\beta v^2 f_0) \right] \end{aligned}$$

$$\begin{aligned}
 & + \frac{m\gamma}{2v^2\tau_b} \frac{\partial}{\partial\mu} \tilde{c}\mu \frac{\partial f_0}{\partial\mu} \\
 \bar{Q}(f_0) = & \frac{1}{\tau_b} \int \frac{dl}{v_{\parallel}} Q(f_0) = \frac{2\pi m q^2}{\tau_b} L_{res} \tilde{q} L_{res} f_0, \quad (1)
 \end{aligned}$$

where

$$\tau_b = \int \frac{dl}{v_{\parallel}}, \quad \tilde{c} = \int \frac{v_{\parallel}}{B} dl,$$

$$\tilde{q} = \sum_{res} \frac{\mu B}{2} \pi \left| \frac{2}{n\dot{\Omega}} \right|^{2/3} Ai^2(x) |\psi_n|^2,$$

$$x = - \frac{(n\dot{\Omega})^2}{4} \left| \frac{2}{n\dot{\Omega}} \right|^{4/3},$$

$$L_{res} = \frac{1}{m} \left(\frac{\partial}{\partial E} + \frac{nq}{m\omega} \right), \text{ and}$$

$$\alpha = \langle \Delta v_{\parallel} \rangle + \frac{1}{2v} \langle (\Delta v_{\perp})^2 \rangle, \quad \beta = \langle (\Delta v_{\parallel})^2 \rangle, \quad \gamma = \langle (\Delta v_{\perp})^2 \rangle,$$

where S is a source or sink term of ions. $\langle \Delta v_{\parallel} \rangle$, $\langle (\Delta v_{\perp})^2 \rangle$, and $\langle (\Delta v_{\perp})^2 \rangle$ are the Coulomb diffusion coefficients, and m and q are the mass and charge of resonant ions, respectively. n is a harmonic number of the ICRF heating. ω and Ω are the applied frequency and the ion cyclotron frequency, respectively. E and μ are the energy and the adiabatic magnetic moment of ions, respectively. The summation of the kick term \sum_{res} is carried out at each resonant point on the magnetic line of force. Airy function is approximated as follows [3]:

$$Ai^2(x) = \begin{cases} \frac{1}{2\pi\sqrt{|x|}} & \text{for } |x| > 0.308 \\ 0.287 & \text{for } |x| < 0.308. \end{cases}$$

The resonance layer exists near the turning point when

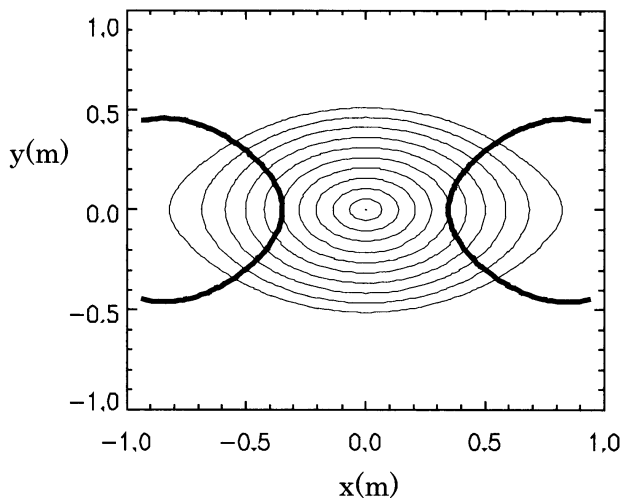


Fig. 1 The helical symmetric plasma model. Bold solid lines indicate the ion cyclotron resonance layer.

$|x| < 0.308$. ψ_n is expressed as follows:

$$\psi_n = \frac{E_{left} J_{n-1}(b) + E_{right} J_{n+1}(b)}{\sqrt{2}},$$

where $b = \frac{k_{\perp} v_{\perp}}{\Omega}$, and E_{left} and E_{right} are left- and right-hand polarized components of the rf electric field, respectively. ψ_n at the cyclotron resonance layer is approximately expressed in the following relation in the case of the second harmonic heating:

$$|\psi_2|^2 \propto J_1^2(b) + 6J_1(b)J_3(b) + 9J_3^2(b).$$

This equation shows that ions are not accelerated in the low energy range, $|\psi_2|^2$ takes the maximum value at $b \approx 3.4$, and the rf kick term vanishes again at $b \approx 6.1$; ions are selectively accelerated in some energy region. Therefore, the higher-energy ions are produced in the higher harmonic heating rather than in the minority heating at the same absorption power.

Ions exist in a triangular region in the μ - E space because of $\mu < E/B_{min}$, where B_{min} is the minimum magnetic field strength along the magnetic line of force. The coordinate is transformed from the μ - E space to the v - ξ space, where v is a velocity of ions and ξ is a cosine of the pitch angle at $B = B_{min}$. The steady state distribution function is obtained by setting the left-hand side of eq. (1) to be zero. In the calculation, only the balance-injection of neutral beam injection (NBI) is considered, then the beam source is symmetry. The sink of NBI particles is located at $v = 0$.

3. Result of calculation

In Fig. 2 is shown the calculated contour plot of the distribution function of ions (H^+) heated by the second harmonic heating. In this case, the normalized minor radius ρ is 0.56,

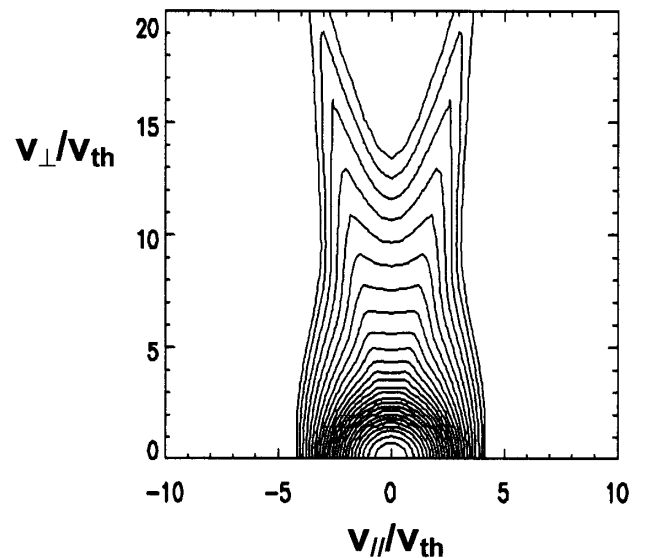


Fig. 2 Contour plot of distribution function at the position of minimum magnetic field on $\rho = 0.56$. The plasma is heated by the second harmonic heating.

the magnetic field strength on axis is 1.325 T, and the frequency is 38.47 MHz, which conditions are similar to those of the experiment. The values employed for electron density and temperature on the axis are $n_{e0} = 1 \times 10^{19} \text{ m}^{-3}$ and $T_{e0} = 2 \text{ keV}$, respectively. The rf electric field strength $|E_0|$ is assumed as 3 kV/m. The ions with a pitch-angle of 82.3° are reflected just at the ion cyclotron resonance layer. The perpendicular velocity of the ion passing through the resonance layer is statistically increased until the reflection point reaches the resonance layer. Therefore, a ‘butterfly’ structure is formed. The solid line in Fig. 3 is the distribution function along the pitch-angle of 82.3° . The ion-energy is found to extend over 3 MeV in this calculated case. The power density is calculated to be 77 kW/m^3 .

There exists a limitation of the maximum energy of ions in the real LHD. Figure 4 shows the confinement limitation obtained by the calculation of the particle-orbit in the LHD [4]. The start point is $\rho = 0.5$, which is on an inner port side of the LHD, with the magnetic field on the axis of

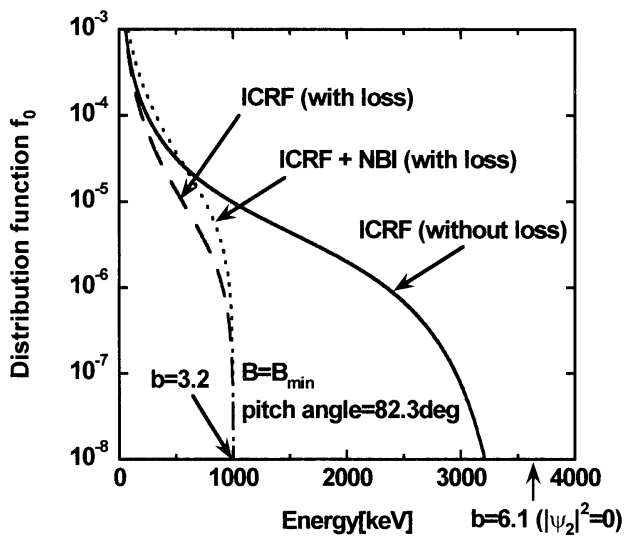


Fig. 3 Three types of distribution functions. The turning points of resonant particles are on the ion cyclotron resonance layer.

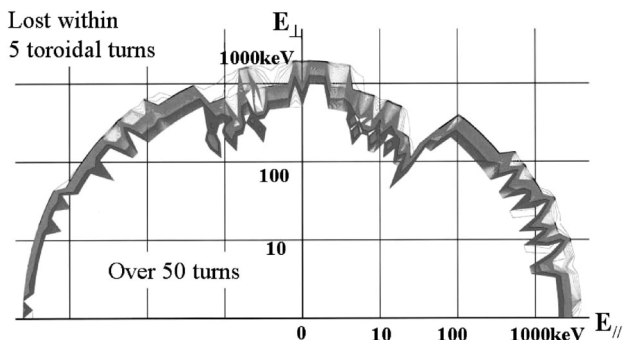


Fig. 4 The boundary of confinement. Outside of this boundary is the region of particle loss.

1.375 T. The confined ion is defined as not-escaped for more than 50 turns in the toroidal direction. The loss boundary is seen at the energy of 1 MeV. Therefore, the loss term $-v_0 H(E - E_c) f_0$ is added to the right-hand side of eq. (1), where H is a Heaviside unit function with E_c of 1 MeV over the whole plasma region. v_0 is employed $1 \times 10^6 \text{ s}^{-1}$ as the loss frequency, which is insensitive to the loss power P_{loss} . Due to the function $H(E - E_c)$, only the particles with energy over 1 MeV are lost. The dashed line in Fig. 3 represents the distribution function calculated with this loss term. The input power is calculated as 70 kW/m^3 , which includes the loss power of 6 kW/m^3 of the resonant ions with an energy over 1 MeV; the net power is reduced to 64 kW/m^3 . When ions with the energy of 150 keV and a pitch angle of 0° are injected from NBI with a power density of 121 kW/m^3 , the tail is enhanced as shown by the dotted line in Fig. 3. P_{loss} is increased to 26 kW/m^3 , and the net power is increased only by 10 % from 64 kW/m^3 to 71 kW/m^3 .

The efficiency of the higher harmonic heating is improved at a higher density, because the loss power can be decreased. Figure 5 shows the distribution functions at the lower and the higher density, i.e., at $n_{e0} = 1 \times 10^{19} \text{ m}^{-3}$ and $n_{e0} = 4 \times 10^{19} \text{ m}^{-3}$, respectively. At the higher density, the tail does not reach 1 MeV as shown by the solid line in Fig. 5 because k_\perp increases with the density, and the energy of 925 keV corresponds to $b = 6.1$ ($|\psi_2|^2 = 0$). Therefore, the lost power is decreased to 0. The power absorption is enhanced and the power density reaches 1 MW/m^3 when the rf field strength is fixed at 3 kV/m. When the power density is fixed at 64 kW/m^3 , then $|E_0|$ decreases to 1 kV/m and the tail shrinks.

In 2001, the second harmonic heating experiment was conducted in the NBI sustained plasma [5]. The absorbed NBI power was 1.5 MW and the injected ICRF power was 2

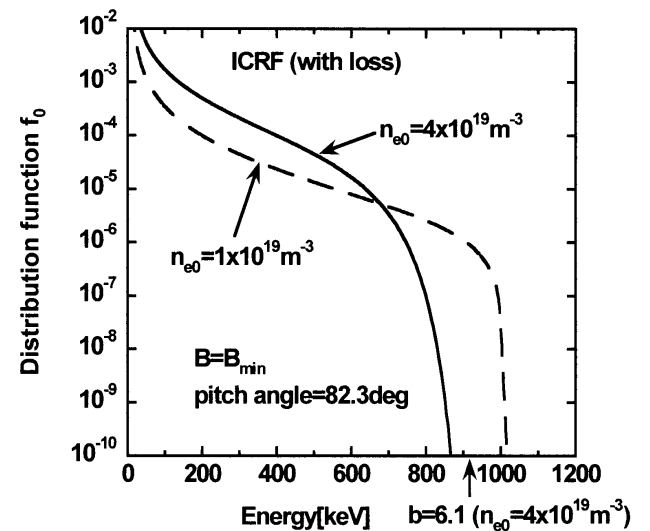


Fig. 5 Distribution functions for different electron densities. The tail of high-density plasma cannot extend over 1 MeV.

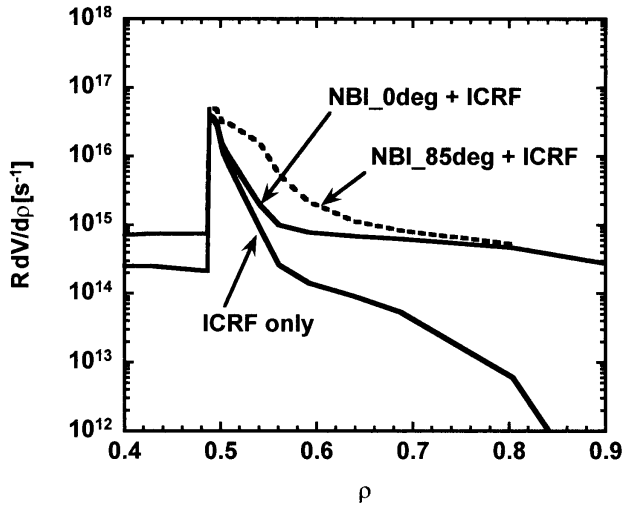


Fig. 6 The profile of the reaction rate. ρ is the normalized minor radius. V is the plasma volume inside ρ .

MW. The net absorbed ICRF power deduced by the decay of the stored energy was 0.6 MW. Using the same plasma parameters as those in the experiment, $n_{e0} = 0.8 \times 10^{19} \text{ m}^{-3}$ and $T_{e0} = 1.2 \text{ keV}$, and, assuming the constant power density of NBI, an effective rf field $|E_0|$ of 3.2 kV/m was deduced. Then the calculated total net power was 0.6 MW and the lost power due to the tail was 0.7 MW. The remaining rf power of 0.7 MW was thought to be absorbed by the unconfined peripheral plasma or the vacuum wall. When the electron density was $4 \times 10^{19} \text{ m}^{-3}$, the calculated loss of the tail decreased to 0.

A D-D reaction rate is also estimated from the calculated distribution function. The conditions are as follows: $|E_0| = 3 \text{ kV/m}$, $f = 38.47 \text{ MHz}$, $B_0 = 2.65 \text{ T}$, $n_{e0} = n_{D0} = 4 \times 10^{19} \text{ m}^{-3}$, $E_c = 1 \text{ MeV}$, and the ion and electron temperature on the axis is 3 keV. Injection energy and power values of the NBI are 50 keV and 4 MW, respectively. These are the values of the

planned perpendicular NBI on LHD. Figure 6 shows the reaction rate of the D-D reaction. ρ is the normalized minor radius and V is the plasma volume inside ρ . The total reaction rate is $5.4 \times 10^{14} \text{ s}^{-1}$ with only the NBI. The additional second harmonic ICRF heating with a net rf power of 1.4 MW would enhance the reaction rate to $1.1 \times 10^{15} \text{ s}^{-1}$ if the NBI was a tangential injection to the torus. The reaction rate is increased to $2.5 \times 10^{15} \text{ s}^{-1}$ by changing the pitch angle of NBI particles from 0 to 85° , and net rf power also increases to 1.9 MW.

4. Summary

The distribution function was calculated for the higher harmonic heating, and the power absorption and the loss of power was estimated using it. In the calculation, a large tail could be formed by second harmonic heating. However, with the low electron density, the high-energy tail was limited within 1 MeV due to particle loss. The population of high-energy ions produced by the ICRF second harmonic heating was increased by the NBI. However, the loss of power was also increased. The loss could be decreased, and the heating power efficiency therefore improved, at the higher density. The D-D reaction rate was calculated from the distribution function. The ICRF heating increased the reaction rate as a result of the high-energy ion tail formation, especially during perpendicular injection of NBI.

References

- [1] T. Mutoh *et al.*, *IAEA Conference 2002*, Lyon, IAEA-EX/P2-19.
- [2] T.H. Stix, *WAVES IN PLASMAS* (AIP, 1992), p521.
- [3] G.W. Hammett, Ph.D. Thesis, Princeton University (1986), p50.
- [4] Y. Matsumoto, S. Oikawa and T. Watanabe, *J. Phys. Soc. Jpn.* **71**, 1684 (2002).
- [5] K. Saito *et al.*, *Plasma Phys. Control. Fusion* **44**, 103 (2002).